Synthesis of $Li[Ni_{1/3}Co_{1/3}Mn_{1/3}]O_{2-z}F_z$ via Coprecipitation

Seung-Taek Myung, Gil-Ho Kim,[†] and Yang-Kook Sun*[†]
VK Corporation, 67 Jije-Dong, Pyongtaek-City, Kyonggi-Do 450-090, Korea
[†]*Department of Chemical Engineering, Hanyang University, Seungdong-Gu, Seoul 133-791, Korea*

(Received July 5, 2004; CL-040794)

$Li[Ni_{1/3}Co_{1/3}Mn_{1/3}]O_{2-z}F_z$ ($z = 0$–0.15) were synthesized via co-precipitation followed by high-temperature heat treatment. From X-ray diffraction investigation, it was found that the as-prepared powders showed the layered $Li[Ni_{1/3}Co_{1/3}Mn_{1/3}]O_{2-z}F_z$ ($z = 0$–0.15) having α-$NaFeO_2$ structure (space group: $R\bar{3}m$). Though the initial discharge capacities of $Li[Ni_{1/3}Co_{1/3}Mn_{1/3}]O_{2-z}F_z$ is somewhat smaller, however, the capacity retention and thermal stability at highly oxidized state were significantly improved comparing to the undoped $Li[Ni_{1/3}Co_{1/3}Mn_{1/3}]O_2$. Fluorine substitution for oxygen made it possible to use the cathode material at 4.6 V cut-off limit.

Lithium transition-metal oxides, $Li[Ni_xCo_{1-2x}Mn_x]O_2$, have received a great deal of interest as rechargeable cathodes for Li-ion secondary batteries.[1] $Li[Ni_{1/3}Co_{1/3}Mn_{1/3}]O_2$ comprises very promising positive electrode materials for high energy and high power lithium-ion batteries.[1] In attempts to increase the reversible capacity of the cathode material, the upper cut-off voltage limit is getting higher. Such a high voltage limit led to obvious increase in the specific discharge capacity. However, $Li[Ni_{1/3}Co_{1/3}Mn_{1/3}]O_2$ has an unstable cycling performance when it cycles up to 4.6 V.[2] The origin of the capacity fading is mainly due to the decaying of electro-active Co ingredient as it was reported by Shaju et al.[2] and Yoon et al.[3]

Metal oxide-coated $LiCoO_2$ showed an enhanced capacity retention above the 4.6-V charge-cutoff voltages comparing to bare $LiCoO_2$, which is probably due to the decreased Co dissolution.[4–6] However, the retention of discharge capacity is not so satisfactory. Another possible approach is to replace oxygen with other elements, such as F and S.[7–13] Fluorine substitution for oxygen in lithium nickelate system was pretty effective to obtain a reduced impedance, lattice changes during cycling and cycling life. Unfortunately, the effect of fluorine in the layered lithium nickelate system was limited to 4.3 V of charge cut-off limit. This paper focuses on the electrochemical properties of F-doped $Li[Ni_{1/3}Co_{1/3}Mn_{1/3}]O_{2-z}F_z$ at higher cut-off voltage limit (4.6 V) and compares their performances with un-substituted $Li[Ni_{1/3}Co_{1/3}Mn_{1/3}]O_2$.

$LiOH{\cdot}H_2O$, $CoSO_4{\cdot}7H_2O$, $NiSO_4{\cdot}6H_2O$, and $MnSO_4{\cdot}H_2O$ were used as starting materials. $[Ni_{1/3}Co_{1/3}Mn_{1/3}](OH)_z$ compounds was synthesized by the co-precipitation method, as reported previously.[14] $Li[Ni_{1/3}Co_{1/3}Mn_{1/3}]O_{2-z}F_z$ was prepared as follows; heating a reaction mixture of the dehydrated $[Ni_{1/3}Co_{1/3}Mn_{1/3}](OH)_x$ and $LiOH{\cdot}H_2O$ and LiF at 1000 °C for 10 h, then subsequent annealing at 700 °C for 5 h in air atmosphere. An excess of lithium was used to compensate for lithium loss during the calcination. Chemical compositions of the resulting powders were analyzed by an atomic absorption spectroscopy (Vario 6, Analyticjena) and an ion chromatography (DX-320, DIONEX, USA) for fluorine.

Powder X-ray diffraction (XRD, Rint-2000, Rigaku, Japan) measurement using Cu Kα radiation was employed to identify the crystalline phase of the synthesized materials. XRD data were obtained $2\theta = 10$ to 80°, with a step size of 0.03° and a count time of 5S. The as-prepared powders were observed using a scanning electron microscope (SEM, JSM 6400, JEOL, Japan). The cathodes were prepared by blending $Li[Ni_{1/3}Co_{1/3}Mn_{1/3}]O_{2-z}F_z$, Super S, carbon black, and polyvinylidene fluoride (80:10:10) in *N*-methyl-2-pyrrolidone. The slurry was then cast on aluminum foil and dried at 110 °C for overnight in vacuum state. Disks were then punched out of the foil. Lithium foil was used as the anode. The electrolyte solution was 1M $LiPF_6$ in a mixture of ethylene carbonate (EC) and diethyl carbonate (DEC) in a 1:1 volume ratio. The cell was assembled in an argon-filled dry box and tested at a current density of 30 mA g^{-1} (0.2 C) at 30 °C. For differential scanning calorimetry (DSC) experiments, the cells were finally fully charged to 4.6 V and opened in the Ar-filled dry box. After opening the cell in the Ar-filled dry box carefully, the extra electrolyte was removed from the surface of the electrode and the electrode materials were recovered from the current collector. A stainless steel-sealed pan with a gold plated copper seal (which can withstand 150 atm of pressure before rupturing and has a capacity of 30 μL) was used to collect 3–5 mg samples. The measurements were carried out in a Pyris 1 Differential Scanning Calorimeter (Perkin Elmer Corporation) using a temperature scan rate of 1 °C min^{-1}, indicating that there were no leaks during the experiments.

For the preparation of $Li[Ni_{1/3}Co_{1/3}Mn_{1/3}]O_2$, the initial LiF amount was always about 2 times of its final composition. That is, for $z = 0.1$ in $Li[Ni_{1/3}Co_{1/3}Mn_{1/3}]O_{2-z}F_z$, 0.9 mol of LiOH and 0.2 mol of LiF were employed against 1 mol of $[Ni_{1/3}Co_{1/3}Mn_{1/3}](OH)_z$. If not, the amount of F was always deficient in the final composition due probably to the evaporation of LiF at 1000 °C. Figure 1 shows X-ray diffraction (XRD) patterns of $Li[Ni_{1/3}Co_{1/3}Mn_{1/3}]O_{2-z}F_z$ with $z = 0$, 0.05, 0.1, 0.15, 0.2, and 0.5, which were calcined at 1000 °C for 10 h in air. All of the peaks can be indexed based on a hexagonal α-$NaFeO_2$ structure. The Li atoms are on 3a sites, the Ni, Co, and Mn atoms are randomly placed on 3b sites, and oxygen and fluorine atoms are on 6c sites. For $Li[Ni_{1/3}Co_{1/3}Mn_{1/3}]O_{2-z}F_z$ ($z = 0.2$, 0.5), the intensities for (003) was analogous to be the (104) peak. But the reflection of (018) and (110) for $Li[Ni_{1/3}Co_{1/3}Mn_{1/3}]O_{2-z}F_z$ are still distinguishable. The resulting XRD peaks are quite narrow, indicating high crystallinity. However, a small impurity peak was observed at around 32° in 2θ. By the combination of atomic absorption and IC analyses for fluorine, the detected F amounts were 0.05, 0.09, and 0.14 for $z = 0.05$, 0.1, and 0.15 in $Li[Ni_{1/3}Co_{1/3}Mn_{1/3}]O_{2-z}F_z$, respectively.

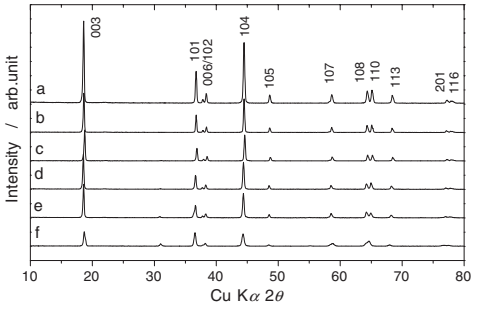

Figure 1. XRD profiles of $Li[Ni_{1/3}Co_{1/3}Mn_{1/3}]O_{2-z}F_z$; (a) $z = 0$, (b) $z = 0.05$, (c) $z = 0.1$, (d) $z = 0.15$, (e) $z = 0.2$, and (f) $z = 0.5$.

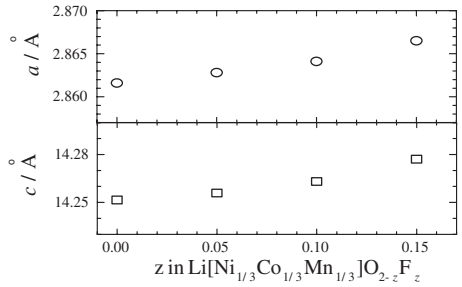

Figure 2. Variation in lattice parameters as a function of F amount in $Li[Ni_{1/3}Co_{1/3}Mn_{1/3}]O_{2-z}F_z$.

Variation in lattice parameters are shown in Figure 2. The lattice parameters were calculated by a least square method from the XRD patterns of Figure 1. Substitution fluorine for oxygen resulted in increase in lattice constant of both *a* and *c* axes. The increase consequently contributes to increase linearly in the unit cell volume. Such a tendency is usually observed in solid solution system, which obeys Vegard's law. In fact, the effective ionic radius of F^- (1.33 Å) is smaller than that of O^{2-} (1.40 Å). Because of the difference in the ionic radius, it was expected that the lattice parameter would decrease by the substitution fluorine for oxygen. Nonetheless, the lattice in both *a* and *c* axes increased. Similar results were also seen in spinel $LiAl_{0.2}Mn_{1.8}O_{4-z}F_z$ system by Amatucci et al.[10] The stronger bond character of Li and F may result in repulsive force in the oxide matrix so that the lattice would expand to both *a* and *c* axes. Therefore, it was found from XRD patterns that a solid solution of $Li[Ni_{1/3}Co_{1/3}Mn_{1/3}]O_{2-z}F_z$ was formed to $z = 0.15$, after which undesired impurity was produced. Detailed structural refinements are currently being carried out.

Figure 3 shows the voltage versus capacity profiles of Li/$Li[Ni_{1/3}Co_{1/3}Mn_{1/3}]O_{2-z}F_z$ cells ($z = 0$–0.15) during 50 cycles. The cells were firstly activated by charging up to 4.6 V and then discharged to 2.8 V by applying a current density of 0.2 C rate (30 mA g^{-1}) at 30 °C. The initial discharge capacity of $Li[Ni_{1/3}Co_{1/3}Mn_{1/3}]O_{2-z}F_z$ decreased with increasing the substitution amount of fluorine. It is likely that the strong covalent bond of Li–F exists in $Li[Ni_{1/3}Co_{1/3}Mn_{1/3}]O_{2-z}F_z$ so that intercalation of Li^+ ions may be perturbed by the strong bond. Observing the discharge curves at the end of discharge, one can clearly see the smooth voltage variation for the F-doped samples, but an abrupt voltage dropping was seen for $Li[Ni_{1/3}Co_{1/3}Mn_{1/3}]O_2$. The F doping also resulted in a small degree of variation in operation voltages; increase in both charge and discharge voltages. This also might be due to the existence of the strong bond by Li–F in the host structure, as the similar behavior was observed by Naghash et al.[9] and Amatucci et al.[10] The high initial discharge capacity of $Li[Ni_{1/3}Co_{1/3}Mn_{1/3}]O_2$ fades gradually on cycling, and finally reaches to 166 mAh g^{-1} after 50

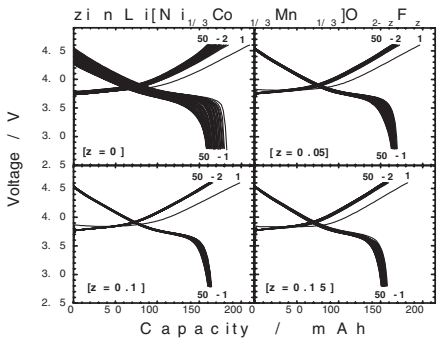

Figure 3. Continuous charge and discharge curves of $Li[Ni_{1/3}Co_{1/3}Mn_{1/3}]O_{2-z}F_z$ ($z = 0$–0.15) at 30 °C.

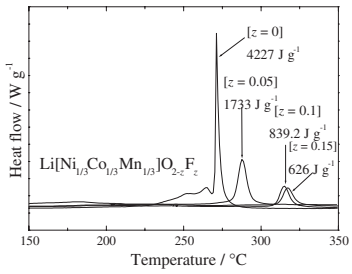

Figure 4. DSC traces of the $Li[Ni_{1/3}Co_{1/3}Mn_{1/3}]O_{2-z}F_z$ at 4.6 V.

cycles. The redox species of $Li[Ni_{1/3}Co_{1/3}Mn_{1/3}]O_2$ are related with $Ni^{2+/4+}$ and $Co^{3+/4+}$. The $Co^{3+/4+}$ redox reaction mainly contributes the higher voltage working, 4.3–4.6 V versus Li^0, which means the Co ingredient was gradually dissolved into the electrolyte by cycling to 4.6 V.[2,3] On the contrast, the Li^+ de-/intercalation processes are highly reversible with small polarization by F-doping in $Li[Ni_{1/3}Co_{1/3}Mn_{1/3}]O_{2-z}F_z$, which demonstrates that whatever the fluorine amounts are the material exhibits good cycling behavior. When $z = 0.1$ in $Li[Ni_{1/3}Co_{1/3}Mn_{1/3}]O_{2-z}F_z$, the best cycling performance was seen due to improved structural stability by F incorporation in the oxygen sites.

Figure 4 shows DSC profiles of wet electrodes of $Li[Ni_{1/3}Co_{1/3}Mn_{1/3}]O_{2-z}F_z$ which were charged to 4.6 V. The DSC experiments were made in welded scaled stainless steel tubes so that no leaking of pressurized electrolyte is possible. As the concentration of fluorine in $Li[Ni_{1/3}Co_{1/3}Mn_{1/3}]O_{2-z}F_z$ increases, the thermal stability of the charged cathode material in electrolyte was greatly improved, even at the small fluorine concentration of 0.05. For fluorine concentration above 0.05 there is about 40 °C increase in the temperature of any significant exothermic activity. The $Li[Ni_{1/3}Co_{1/3}Mn_{1/3}]O_2$ is a large peak between 234 and 283 °C, and it produces 4227 J g^{-1} of heat. When the fluorine amount increases, $Li[Ni_{1/3}Co_{1/3}Mn_{1/3}]O_{2-z}F_z$ has a small peak between 311 and 328 °C, also it only produces 626 J g^{-1} of heat generation, even though the electrode is highly oxidized state. Therefore, it is able to conclude that $Li[Ni_{1/3}Co_{1/3}Mn_{1/3}]O_{2-z}F_z$ with $z = 0.05$, 0.1, 0.15 is safer than $Li[Ni_{1/3}Co_{1/3}Mn_{1/3}]O_2$. From the results of rate capability, cycling, and DSC tests, the fluorine substitution for oxygen in $Li[Ni_{1/3}Co_{1/3}Mn_{1/3}]O_2$ provides the improved structural and thermal stability and it consequently results in enhancement of electrochemical properties and safety concern.

This research was supported by University IT Research Center Project.

References

1 D. D. MacNeil, Z. Lu, and J. R. Dahn, *J. Electrochem. Soc.*, **149**, A1332 (2002).
2 K. M. Shaju, G. V. Subba Rao, and B. V. R. Chowdari, *Electrochim. Acta*, **48**, 145 (2002).
3 W.-S. Yoon, C. P. Grey, M. Balasubramanian, X.-Q. Yang, and J. McBreen, *Chem. Mater.*, **15**, 3161 (2003).
4 A. M. Kannan, L. Rabenberg, and A. Manthiram, *Electrochem. Solid-State Lett.*, **6**, A16 (2003).
5 Z. Chen and J. R. Dahn, *Electrochem. Solid-State Lett.*, **5**, A213 (2002).
6 J.-G. Lee, B. Kim, J. Cho, Y.-W. Kim, and B. Park, *J. Electrochem. Soc.*, **151**, A801 (2004).
7 K. Kudo, S. Arai, S. Yamada, and M. Kanda, *J. Power Sources*, **81–82**, 599 (1999).
8 A. R. Naghash and J. Y. Lee, *Electrochim. Acta*, **46**, 941 (2001).
9 A. R. Naghash and J. Y. Lee, *Electrochim. Acta*, **46**, 2293 (2001).
10 G. G. Amatucci, N. Pereira, T. Zheng, and J.-M. Tarascon, *J. Electrochem. Soc.*, **148**, A171 (2001).
11 P. S. Whitfield and I. J. Davidson, *J. Electrochem. Soc.*, **147**, 4476 (2000).
12 Y.-K. Sun, Y.-S. Jeon and H.-J. Lee, *Electrochem. Solid-State Lett.*, **3**, 7 (2000).
13 S.-H. Park, K.-S. Park, Y.-K. Sun, and K.-S. Nahm, *J. Electrochem. Soc.*, **147**, 2116 (2000).
14 M.-H. Lee, Y.-J. Kang, S.-T. Myung, and Y.-K. Sun, *Electrochim. Acta*, in press.

Published on the web (Advance View) September 25, 2004; DOI 10.1246/cl.2004.1388